Journal of Visualized Experiments

Analyzing the α-Actinin Network in Human iPSC-Derived Cardiomyocytes Using Single Molecule Localization Microscopy

--Manuscript Draft--

Article Type:	Invited Methods Article - JoVE Produced Video
Manuscript Number:	JoVE61605R1
Full Title:	Analyzing the α-Actinin Network in Human iPSC-Derived Cardiomyocytes Using Single Molecule Localization Microscopy
Section/Category:	JoVE Biology
Keywords:	Human induced pluripotent stem cells; super resolution; Maturation; sarcomere network; photoactivated localization microscopy; cardiomyocyte
Corresponding Author:	Heiko Lemcke Universitatsmedizin Rostock Rostock, GERMANY
Corresponding Author's Institution:	Universitatsmedizin Rostock
Corresponding Author E-Mail:	heiko.lemcke@uni-rostock.de;voronina.natali12@gmail.com
Order of Authors:	Lisa Johann
	Cajetan Immanuel Lang
	Oleksandra Chabanovska
	Robert David
	Heiko Lemcke
Additional Information:	
Question	**Response**
Please indicate whether this article will be Standard Access or Open Access.	Standard Access (US$2,400)
Please indicate the **city, state/province, and country** where this article will be **filmed**. Please do not use abbreviations.	Rostock, Germany

TITLE:

Analyzing the α-Actinin Network in Human iPSC-Derived Cardiomyocytes Using Single Molecule Localization Microscopy

AUTHORS AND AFFILIATIONS:

Lisa Johann[1,2], Oleksandra Chabanovska[1,2], Cajetan Immanuel Lang[3], Robert David[1,2], Heiko Lemcke[1,2]

[1]Department of Cardiac Surgery, Reference and Translation Center for Cardiac Stem Cell Therapy (RTC), Rostock University Medical Center, Rostock, Germany
[2]Faculty of Interdisciplinary Research, Department Life, Light & Matter, University Rostock, Rostock, Germany
[3]Department of Cardiology, Rostock University Medical Center, Rostock, Germany

Corresponding author:
Robert David (robert.david@med.uni-rostock.de)

Email addresses of co-authors:
Heiko Lemcke (heiko.lemcke@med.uni-rostock.de)
Oleksandra Chabanovska (oleksandra.chabanovska@uni-rostock.de)
Lisa Johann (lisa.johann@med.uni-rostock.de)
Cajetan Immanuel Lang (cajetan.lang@med.uni-rostock.de)
Robert David (Robert.david@med.uni-rostock.de)

KEYWORDS:

human induced pluripotent stem cells, cardiomyocyte, super resolution, maturation, sarcomere network, photoactivated localization microscopy

SUMMARY:

The formation of a proper sarcomere network is important for the maturation of iPSC-derived cardiomyocytes. We present a super resolution-based approach that allows for the quantitative evaluation of the structural maturation of stem cell derived cardiomyocytes, to improve culture conditions promoting cardiac development.

ABSTRACT:

The maturation of iPSC-derived cardiomyocytes is a critical issue for their application in regenerative therapy, drug testing and disease modeling. Despite the development of multiple differentiation protocols, the generation of iPSC cardiomyocytes resembling an adult-like phenotype remains challenging. One major aspect of cardiomyocytes maturation involves the formation of a well-organized sarcomere network to ensure high contraction capacity. Here, we present a super resolution-based approach for semi-quantitative analysis of the α-actinin network in cardiomyocytes. Using photoactivated localization microscopy a comparison of sarcomere length and z-disc thickness of iPSC-derived cardiomyocytes and cardiac cells isolated from neonatal tissue was performed. At the same time, we demonstrate the importance of

proper imaging conditions to obtain reliable data. Our results show that this method is suitable to quantitatively monitor the structural maturity of cardiac cells with high spatial resolution, enabling the detection of even subtle changes of sarcomere organization.

INTRODUCTION:

Cardiovascular diseases (CVD) such as myocardial infarction or cardiomyopathy remain the major cause of death in the western world[1]. As the human heart possesses only poor regenerative capacity, there is a need for strategies to promote the recovery from CVDs. This includes cell replacement therapies to replenish lost cardiomyocytes (CM), as well as the development of new anti-arrhythmic drugs for efficient and safe pharmaceutical intervention. Induced pluripotent stem cell (iPSC) have been shown to be a promising cell source for the unlimited generation of human CM in vitro, suitable for regenerative therapies, disease modeling, and for the development of drug screening assays[2–4].

Although many different cardiac differentiation protocols exist, iPSC-derived CM still lack certain phenotypical and functional aspects that impede the in vitro and in vivo application[5,6]. Beside electrophysiologic, metabolic, and molecular changes, the cardiac maturation process involves the structural organization of sarcomeres, which are the fundamental units required for force generation and cell contraction[7]. While adult CMs exhibit a well-organized contractile apparatus, iPSC-derived CMs commonly demonstrate disarranged sarcomere filaments, associated with a reduced contraction ability and altered contraction dynamics[8,9]. In contrast to mature CM that show uniaxial contraction pattern, the disoriented structures in immature CM results in a radial contraction of the whole cell or promote the appearance of contraction focal points[9,10].

For improving cardiac maturation, multiple approaches have been applied, including 3D cell culture methods, electrical and mechanical stimulation, as well as the use of extracellular matrices mimicking in vivo conditions[11–13]. To evaluate the success and efficiency of these different culture conditions, techniques are needed to monitor and estimate the degree of the structural maturation of iPSC CM, e.g., by microscopic techniques. In contrast to conventional confocal imaging, the resolution in case of photoactivated localization microscopy (PALM) is approximately 10x higher. This technique in turn allows for a more accurate analysis, detecting even subtle alterations of cellular structures[14]. Considering the high resolution of PALM-based imaging, the overall goal of this method was the microscopic evaluation of sarcomere maturity in iPSC-derived CMs by precise determination of z-Disc thickness and sarcomere length. In previous studies, these structural features have been shown to be appropriate parameters to assess cardiac maturity[15]. For example, diseased iPSC-CM lacking full length dystrophin exhibit reduced sarcomere length and z-band width when compared to wild type cells[16]. Likewise, the length of individual sarcomeres was measured to investigate the impact of topographic cues on cardiac development[16]. Hence, we applied this approach to evaluate the structural maturation of the sarcomere network in iPSC-CM by quantitatively measuring the sarcomere length and z-disc thickness.

PROTOCOL:

All steps in this protocol involving neonatal and adult mice were performed according to the ethical guidelines for animal care of the Rostock University Medical Centre.

1. Cultivation and dissociation of iPSC-derived cardiomyocytes

1.1. Differentiate hiPSC-CMs for 25 days using a 2D monolayer method as described previously[17].

1.2. Prewarm dissociation medium to 37 °C and support medium to room temperature.

1.3. Wash cells twice with PBS.

1.4. Add prewarmed dissociation medium to cells and incubate for 12 min at 37 °C and 5% CO_2.

1.5. Add support medium to the cells.

NOTE: The volume of added support medium needs to be twice the volume of dissociation medium used in step 1.4.

1.6. Dislodge the cells using a 5 mL serological pipette.

1.7. Centrifuge cells at 200 *x g* for 5 min and resuspend the pellet in 3 mL of hiPSC-CM culture medium[17].

1.8. Seed cells in 8 well glass bottom chambers at a cell density of 75,000 cells/well and culture for 3 days.

2. Adult cardiomyocyte isolation

2.1. Isolation and cultivation of adult cardiomyocytes from NMRI mice was performed as reported previously[18].

2.2. Seed cells in 8 well glass chamber slide and culture for one day.

3. Isolation and cultivation of neonatal cardiomyocytes

3.1. Isolation procedure of neonatal cardiomyocytes, obtained from NMRI mice, was performed as described previously[19].

3.2. Seed isolated cell in 8 well glass chamber slide at a cell density of 75,000 cells/well and culture for 3 days in neonatal CM culture medium[19].

4. Immunofluorescence labeling of the α-actinin network

NOTE: For optimal results, cells are cultured in 8 well glass bottom chambers. Labeling should be performed one day before imaging.

4.1. Prewarm 4% PFA at 37 °C.

4.2. Fix iPSC-CM by adding 4% paraformaldehyde directly into the culture media (1:1 dilution) and incubate at 37 °C for 15 min. The final concentration of PFA for fixation is 2%.

4.3. Incubate fixed cells in 0.2% Triton-X, diluted in PBS, for 5 min at room temperature.

4.4. Wash cells twice with PBS, 5 min each.

4.5. Add 1% BSA solution (diluted in PBS) and incubate for 60 min at room temperature.

4.6. Prepare 150 µL of primary antibody solution by diluting α-actinin antibody 1:100 in 1% BSA, containing 0.05% Triton-X. Add to cells and incubate at room temperature for 60 min.

4.7. Wash cells twice with 0.2% BSA solution, 5 min each.

4.8. Prepare 150 µL of secondary antibody solution by diluting goat-anti-mouse Alexa647 antibody 1:100 in 1% BSA, containing 0.05% Triton-X. Add to the cells and incubate at room temperature for 40 min.

4.9. Wash cells twice with 0.2% BSA solution, 5 min each.

4.10. Wash cells twice with PBS, 5 min each. Keep labeled cells in the dark at 4 °C until PALM imaging.

5. Preparation of the PALM imaging buffer

NOTE: It is critical to freshly prepare the PALM imaging buffer for each experiment.

5.1. Prepare 50% glucose solution by dissolving 25 g glucose in 50 mL of distilled water.

5.2. Prepare basic buffer containing 50 mM Tris-HCl, 10% glucose and 10 mM sodium chloride.

5.2.1. Adjust the pH level to ~8.0 using hydrochloric acid.

5.3. Prepare pyranose oxidase solution by dissolving 0.6 mg pyranose oxidase in 316 µL of basic buffer.

5.4. Prepare catalase solution by dissolving 7 mg of catalase in 500 µL of basic buffer. Mix thoroughly and centrifuge at 10,000 *x g* for 3 min. Keep the supernatant for further use. Catalase solution can be kept at 4 °C for several days.

5.5. Prepare 500 µL of PALM imaging buffer by mixing 316 µL of pyranose oxidase solution, 25 µL of catalase solution, 100 µL of 50% glucose solution, 50 µL of cysteamine, 5 µL of cyclooctatetraene and 3.5 µL of β-Mercaptoethanol. The final catalytic activity of pyranose oxidase and catalase need to be 7.5 U, 35,00U respectively.

NOTE: The PALM imaging buffer provides optimal imaging conditions for 3-5 h. If blinking capability of the fluorescent dye decreases, prepare a new buffer aliquot.

6. PALM image acquisition

6.1. Switch on the microscope at least 3 h before use and bring the sample to room temperature before imaging to allow thermal equilibration. If the microscope is equipped with an incubation chamber, adjust temperature to 30 °C.

6.2. Clean the objective and bottom of the chamber slide using an appropriate cleaning solvent.

6.3. Add 300 µL of PALM imaging buffer into one well of labeled cells and insert the chamber slide into the stage holder of the microscope.

6.4. Set the PALM image acquisition parameters.

6.4.1. Select 1.57 N.A. 100x oil objective for acquisition.

6.4.2. Select PALM mode and activate the TIRF settings.

6.4.3. Adjust the number of frames to be acquired. Usually 5, 000-10, 000 frames are sufficient to obtain optimal results. However, the number of acquired frames strongly depends on the labeling efficiency and the blinking capability of the fluorescent dye and may be adjusted by the user.

6.4.4. Set UV laser power to 0.1% and 647 laser to 0.2%.

6.4.5. Set the gain level to 50-100.

6.4.6. Switch on the laser illumination and select a target cell. The gain level can be increased if signal intensity is to low (depending on fluorescence labeling).

6.4.7. Switch off the laser illumination

6.5. PALM image acquisition

6.5.1. Reduce gain to 0 and increase the laser power (ex 647) to 100%.

6.5.2. Bleach the target cell for ~5 s.

6.5.3. Increase gain to 50 and start PALM image acquisition.

NOTE: Gain needs to be adjusted to get sufficient signal intensity while oversaturated pixels should be avoided. If signal intensity reduces, increase the gain level.

6.6. Optionally, steadily enhance the UV laser power (0.1%-10%) to increase signal intensity and to promote blinking of the fluorophore.

7. Reconstruction of PALM data

7.1. Open the Image J software and import PALM data.

7.2. Open Thunderstorm Plugin and "**Run analysis**"

7.2.1. In the "**Camera setup**" menu enter pixel size and EM gain.

NOTE: When using 100x objectives and 1.6x magnification lens, 100 nm pixel size is appropriate. However, as the pixel size depends on the hardware features of the microscope and camera used for PALM imaging, users need to carefully check and adapt this parameter. EM gain values can be obtained from the metadata.

7.2.2. In the "**Run analysis menu**" set parameters as follows: B-spline order: 3, B-spline scale: 2.0, peak intensity threshold: stf(Wave.F1), fitting radius: 3, initial sigma: 1.6, magnification: 5.0, update frequency: 50, lateral shifts: 2. Confirm by clicking the "**Ok**" button.

7.3. Post processing of reconstructed PALM image

7.3.1. In the "**Plot histogram**" menu select the "**Sigma**" parameter.

7.3.2. Use the "**Rectangle**" tool to select a ROI, excluding possible artefacts and apply ROI to the filter. ROI values will appear in the filter command box.

7.3.3. Add "**& uncertainty <25**" to the ROI values. A possible filter command will look like this: "(sigma > 48.6821 & sigma < 1117.40) & uncertainty <25". Apply selected sigma values.

7.3.4. In the "**Remove duplicates**" menu, enter a distance threshold of "10 nm" and apply.

7.3.5. In the "**Merging menu**", set maximum distance to "20", maximum frames per molecule

to “0” and maximum off frames to “1”. Apply settings.

7.3.6. In the “**Drift correction menu**”, select cross correlation and set “**Number of bins**” to “5” and “**Magnification**” to “5.0”. Apply drift correction settings.

7.3.7. Save the final PALM image and export post processed data if desired.

8. Analysis of sarcomere filaments

8.1. Analysis of sarcomere length

8.1.1. Open Image J software and import the reconstructed PALM image.

8.1.2. Draw a line between selected sarcomere structures perpendicular to the z-disc to measure the shortest distance between actinin filaments.

8.1.3. Select “**Plot profile**” in the “**Analyze**” menu and acquire the length between two peaks. As sarcomere length may vary within one cell, a minimum of 20 sarcomeres should be measured in different areas of the target cell.

8.2. Analysis of z-Disc thickness

8.2.1. Open Image J software and import the reconstructed PALM image.

8.2.2. Convert the reconstructed PALM image into an 8-bit mode image.

8.2.3. Open the ridge detection plugin and enter the following parameters: line width: 20, high contrast: 230, low contrast: 10, sigma: 0.79, lower threshold: 25.84, minimum line length: 20.

8.2.4. Set “**Estimate width**”, “**Extend line**” and “**Display results**”.

8.2.5. Click “**Ok**” and use “**Mean line width**” from results table for further analyses.

REPRESENTATIVE RESULTS:

For estimating the degree of structural maturation of CM, neonatal, fully mature adult, and iPSC CM were initially labeled the CM with α-actinin antibody to visualize the sarcomere network. Following PALM acquisition, images were reconstructed, and z-disc thickness was measured using plugin-based image processing software for the automatic detection of the width of individual filaments. Sarcomere length was calculated by measuring the distance between two adjacent intensity peaks, corresponding to neighboring filaments. **Figure 1** shows the evaluation of the sarcomere organization in iPSCs-derived CM.

As presented in **Figure 2A**, iPSC-CM and neonatal cells were found to exhibit a similar α- actinin pattern with irregular, disarranged sarcomere structures. Likewise, quantitative assessment

demonstrated that the length and thickness of α- actinin filaments were almost identical which indicates a premature developmental state of iPSC CM. More precisely, the average sarcomere length was about 1.83 µm (adult vs. iPSC CM vs. neonatal CM: 1.91 ± 0.02 1.83 ± 0.049 µm vs. 1.82±0.03 µm, n=20 cells), while z-Disc thickness was approximately 74 nm (adult vs. iPSC CM vs. neonatal CM: 71.30 ± 1.64 vs. 73.95 ± 0.86 nm vs. 74.08 ± 0.12 nm, n=20 cells) (**Figure 2B**). In contrast, adult mature CM showed a regular sarcomere network with slightly increased sarcomere length and reduced z-Disc thickness.

Comparison of conventional confocal imaging and PALM demonstrated no significant difference of sarcomere length (**Figure 2C**) (confocal vs. PALM: 1.75 ± 0.02 vs. 1.70 ± 0.02, n=10 cells). However, a profound reduced z-Disc thickness was detected when iPSC-CM were subjected to PALM imaging (**Figure 2C**) (confocal vs. PALM: 224.71 ± 4.31 vs. 73.91 ± 1.31, n=10 cells). Representative images highlight the gain in resolution when PALM was applied, supported by corresponding intensity plots (**Figure 2D,E**). Calculated full width at half maximum of fluorescence intensity revealed that α-actinin structures are ~3-fold thinner in PALM images if compared to standard confocal microscopy (**Figure 2E**).

Single molecule localization microscopy, like PALM, enables the detection of intracellular structures far below the diffraction limit. To ensure maximum spatial resolution, appropriate imaging conditions are required for precise detection of single molecule localization. The used imaging buffer system is critical for this acquisition process as it influences the photophysical properties of the fluorescent dye and, thus, has a significant impact on the overall resolution and accuracy of the final PALM image. Comparison between high quality buffer and buffer prepared one day before imaging revealed a profound difference in filament thickness (**Figure 3A,B**). Sarcomere structures acquired with low quality buffer appear to be thicker when compared to optimal imaging conditions (**Figure 3A**). Indeed, quantitative evaluation showed that z-Disc thickness was increased by ~65% (high quality vs. low quality: 73.87 ± 1.02 nm vs. 113.9 ± 1.33 nm, n=155 filaments) (**Figure 3B**). This lack of data accuracy is due to reduced blinking properties of the fluorophore that results in less detected photons per localization event (high vs. low buffer quality: 29689 photons/event vs. 16422 photons/events) (**Figure 3C**). Moreover, localization precision is decreased under deteriorated imaging conditions (high quality vs. low quality: 14.25 ± 5.85 nm vs. 19.56 ± 6.7 nm), which lowers overall resolution of the reconstructed PALM image (**Figure 3C**).

In addition, sample drift, e.g., caused by thermal instability, can affect precise localization of fluorescent molecules and results in blurry images, as presented in **Figure 3D**. While optimal PALM imaging gives clear and well-defined intensity peaks, excessive sample drift produces an irregular intensity pattern that makes it difficult to accurately determine the distance between two adjacent filaments. These data highlight the importance of tightly controlled imaging conditions in single molecule localization microscopy as even subtle changes during the acquisition process can dramatically decrease image quality and data accuracy.

FIGURE AND TABLE LEGENDS:

Figure 1: Evaluation of the sarcomere organization in iPSCs-derived CM. The sarcomere network was fluorescently labeled with an α-actinin antibody, followed by PALM image acquisition. Subsequent reconstruction leads to the final PALM image that was used for quantitative analysis. The length of individual sarcomeres was determined by measuring the distance between two intensity peaks corresponding to neighboring sarcomere filaments (1-5). Z-Disc thickness was automatically calculated by a plugin-based image processing tool. Scale bar 10 µm.

Figure 2: Quantitative comparison of z-disc thickness and sarcomere length in CM derived from iPSCs, adult, and neonatal heart tissue. (**A**) Reconstructed PALM images of the α-actinin network of iPSC and neonatal CM. (**B**) Quantitative assessment revealed that all neonatal and share high similarity in sarcomere length (adult vs. iPSC CM vs. neonatal CM: 1.91 ± 0.02 1.83 ± 0.049 µm vs. 1.82±0.03 µm) and thickness of individual filaments (adult vs. iPSC CM vs. neonatal CM: 71.30 ± 1.64 vs. 73.95 ± 0.86 nm vs. 74.08 ± 0.12 nm), indicating the premature phenotype of iPSC CM. (**C**) Comparison of sarcomere length and z-Disc thickness between conventional confocal imaging and PALM-based data acquisition. As sarcomere length was determined by measuring the peak-to-peak distance, the impact of increased resolution on data accuracy was less pronounced (confocal vs. PALM: 1.75 ± 0.02 vs. 1.70 ± 0.02). In contrast, a significantly lower z-Disc thickness was detected when PALM was applied (confocal vs. PALM: 224.71 ± 4.31 vs. 73.91 ± 1.31). (**D**) Representative microscopic images of iPSC-CM obtained by confocal and PALM imaging. (**E**) Fluorescence intensity plots corresponding to the red line shown in (D). Values represent full width at half maximum of fluorescence intensity, indicating a profound increase of resolution in PALM images. Data are presented as mean ± SEM, n=10-20 cells, 20 sarcomeres per cell were evaluated. Statistical significance was determined using students *t*-Test. **p<0.005, Scale bar 10 µm.

Figure 3: Impact of buffer quality and sample drift on data accuracy and reliability. (**A**) Representative PALM images of iPSC-derived CM acquired under different imaging conditions. Sarcomere filaments appear thicker in samples that have been imaged with buffer of low quality. Red lines indicate representative measurement of sarcomere length, while green filament structures were included into z-Disc analysis. (**B**) Quantitative evaluation confirmed a significant difference in z-Disc thickness between low- and high-quality buffer (high vs. low buffer quality: 73.87 ± 1.02 nm vs. 113.9 ± 1.34 nm) (**C**) This difference in image accuracy was based on a reduced blinking capability of the fluorophore, leading to a reduced number of detected photons per molecule (high vs. low buffer quality: 29689 photons/event vs. 16422 photons/events). At the same time, localization precision decreased which in turn lowered overall resolution (high vs. low buffer quality: 14.25 ± 5.85 vs. 19.56 ± 6.7) (**D**) Likewise, excessive sample drift can impair image quality. While proper image acquisition without sample drift results in well-defined intensity peaks of α-actinin filaments, increased sample drift provokes an irregular intensity pattern, which strongly affects accurate analysis of sarcomere length. Data are presented as mean ± SEM. 155 filaments were analyzed. Statistical significance was determined using students *t*-Test. ****p<0.0001. Scale bar 10µm.

DISCUSSION:

The generation of functional iPSC-derived CM in vitro is important for regenerative therapies, disease modeling and the development of drug-screening platforms. However, insufficient maturity of these CM is a major obstacle in cardiovascular research[20]. In this regard, high resolution imaging techniques are needed that enable monitoring of the structural maturation state of iPSC-derived CM. At the same time, super resolution microscopy can be a valuable tool to precisely analyze the function of specific proteins, required for proper sarcomere formation as recently demonstrated for titin and troponin[10,21,22].

In the current protocol, we present a PALM-based approach to quantitatively evaluate the structural maturation of iPSC CM by analyzing the α-actinin sarcomere network.

Compared to the conventional light microscopy, PALM enables visualization of cellular structures with a resolution of ~20-50 nm[23]. Thus, it allows detecting even subtle alterations of the cardiac sarcomere network that are barely or not even detectable by classical light microscopy approaches. Applying PALM, we have measured an average sarcomere length of ~1.84 µm in iPSC and neonatal CM (**Figure 2**). This is in line with several previous reports showing that the size of individual sarcomeres is ~1.7-2.0 µm[24–26]. Compared to sarcomere length, precise estimation of the thickness of z-lines is more complicated as its size is far below the classical resolution limit of light microscopy. Using electron microscopy, previous studies revealed that z-Disc thickness ranges from 50 to 80 nm in iPSC CM, which is similar to our PALM-based detection of ~73 nm (**Figure 2**).

Comparison with standard confocal microscopy demonstrated the dramatic increase in resolution when PALM was applied. We found a 3-fold lower z-Disc thickness, following PALM imaging (**Figure 2**). However, no significant difference was measured for the sarcomere length. Since this parameter is measured by detecting the peak-to-peak distance of intensity plots, the effect of increased resolution is less pronounced.

To achieve this high spatial resolution, PALM requires well-defined imaging conditions that need to be carefully addressed by the user. For an accurate localization of single molecules, fluorophores are needed that possess special photophysical properties, enabling rapid switching between fluorescent and dark state, called blinking[27]. As previously demonstrated, the selection of fluorophores can strongly affect image quality[28]. A profound blinking capability was described for Alexa 647, one of the best and widely used dyes for single molecule localization microscopy[29–31]. However, since numerous PALM fluorophores are available, users will have high flexibility in terms of sample labelling[27, 28].

Besides selection of suitable fluorophore, the imaging buffer system is another critical point in PALM imaging as it dictates the photophysical properties of the fluorescent dye. We have applied pyranose oxidase as an oxygen scavenger system that is superior to glucose oxidase as it provides an increased pH stability, hence, allowing long-term imaging without a significant decrease of fluorophore blinking over time[32,33]. Yet, as the lifetime of the imaging buffer is limited to several hours, it must be freshly prepared for each experiment to ensure high

reproducibility. Our results demonstrate a dramatic decrease of data accuracy following PALM imaging with low quality buffer, leading to impaired blinking capability and reduced localization precision (**Figure 3A-C**).

Moreover, thermal stability of the imaging system is mandatory to avoid increased sample drift. While moderate drift can be corrected by computational analysis, excessive sample movement leads to miscalculated localization of detected fluorophores and reduces image quality and data accuracy. This can be prevented by using microscopes with heating chambers and sufficient thermal equilibration of the respective sample before starting PALM imaging. In addition, labeling density and efficiency as well as the use of antibody fragments or nanobodies should be considered to optimize imaging conditions[34–36].

The acquisition process of large cellular structures may take 10-30 min, depending on the imaging parameters (field of view, fluorescent probe, imaging buffer etc.). This long acquisition time is a drawback of PALM which makes it less appropriate for live cell imaging. Typically, 5.000-10.000 frames are captured to achieve an adequate number of blinking events with high localization precision. Also, the imaging depth is usually limited to few hundred nanometers, which makes it difficult to investigate thicker samples. However, enhanced resolution in z-direction can be obtained with a 3D PALM setup[37].

We have selected two parameters to characterize the α-actinin network of iPSC CM, including sarcomere length and z-Disc thickness. Additional features could be collected to get a more comprehensive view on the sarcomere scaffold, such as filament orientation. Likewise, 3D PALM can help to quantitatively analyze the whole sarcomere structure by estimation of present nodes and branches within the network.

Although PALM enables a very detailed analysis of the sarcomere structure, this method does not allow the acquisition of functional parameters like cellular contractility, which is another important feature to evaluate cardiac maturity. Former reports have shown that microscopy-based assessment of sarcomere structure can be combined with video analysis to obtain functional data[38,39]. However, since the authors have used conventional fluorescence microscopy obtained data about the sarcomere structure are less accurate if compared with PALM. Our approach also provides the possibility to correlate PALM data with previous time lapse recordings and therefore allows the acquisition of contraction measurements.

In summary, this protocol provides a method to quantitatively evaluate the structural maturation of the sarcomere network in CM. Using this super resolution-based approach, strategies can be establish targeting an improved cardiac development of iPSC-derived CM to obtain a more adult-like phenotype.

ACKNOWLEDGMENTS:
This study was supported by the EU structural Fund (ESF/14-BM-A55-0024/18). In addition, H.L. is supported by the FORUN Program of Rostock University Medical Centre (889001 and 889003) and the Josef and Käthe Klinz Foundation (T319/29737/2017). C.I.L. is supported by the

Clinician Scientist Program of the Rostock University Medical Center. R.D is supported by the DFG (DA1296/6-1), the DAMP foundation, the German Heart Foundation (F/01/12) and the BMBF (VIP+ 00240).
We thank Madeleine Bartsch for her technical support in iPSC cell culture and cardiac differentiation.

DISCLOSURES:

The authors declare no conflict of interest.

REFERENCES:

1. McAloon, C. J. et al. The changing face of cardiovascular disease 2000–2012: An analysis of the world health organisation global health estimates data. *International Journal of Cardiology*. **224**, 256–264 (2016).
2. Kussauer, S. David, R., Lemcke, H. hiPSCs Derived Cardiac Cells for Drug and Toxicity Screening and Disease Modeling: What Micro- Electrode-Array Analyses Can Tell Us. *Cells*. **8** (11), 1331 (2019).
3. Ylä-Herttuala, S. iPSC-Derived Cardiomyocytes Taken to Rescue Infarcted Heart Muscle in Coronary Heart Disease Patients. *Molecular Therapy*. **26** (9), 2077 (2018).
4. Kadota, S., Shiba, Y. Pluripotent Stem Cell-Derived Cardiomyocyte Transplantation for Heart Disease Treatment. *Current Cardiology Reports*. **21** (8), 73 (2019).
5. Jiang, Y., Park, P., Hong, S. M., Ban, K. Maturation of cardiomyocytes derived from human pluripotent stem cells: Current strategies and limitations. *Molecules and Cells*. **41** (7), 613–621 (2018).
6. Feric, N. T., Radisic, M. Maturing human pluripotent stem cell-derived cardiomyocytes in human engineered cardiac tissues. *Advanced Drug Delivery Reviews*. **96**, 110–134 (2016).
7. Ali, H., Braga, L., Giacca, M. Cardiac regeneration and remodelling of the cardiomyocyte cytoarchitecture. *The FEBS Journal*. **287** (3), 417–438 (2020).
8. Yang, X., Pabon, L., Murry, C. E. Engineering adolescence: maturation of human pluripotent stem cell-derived cardiomyocytes. *Circulation Research*. **114** (3), 511–23 (2014).
9. Bedada, F. B., Wheelwright, M., Metzger, J. M. Maturation status of sarcomere structure and function in human iPSC-derived cardiac myocytes. *Biochimica et Biophysica Acta - Molecular Cell Research*. **1863** (7), 1829–1838 (2016).
10. Dai, Y. et al. Troponin destabilization impairs sarcomere-cytoskeleton interactions in iPSC-derived cardiomyocytes from dilated cardiomyopathy patients. *Scientific Reports*. **10** (1), 1–15 (2020).
11. Huang, C. Y. et al. Enhancement of human iPSC-derived cardiomyocyte maturation by chemical conditioning in a 3D environment. *Journal of Molecular and Cellular Cardiology*. **138**, 1–11 (2020).
12. Ronaldson-Bouchard, K. et al. Advanced maturation of human cardiac tissue grown from pluripotent stem cells. *Nature*. **556** (7700), 239–243 (2018).
13. Lee, S. et al. Contractile force generation by 3D hiPSC-derived cardiac tissues is enhanced by rapid establishment of cellular interconnection in matrix with muscle-mimicking stiffness. *Biomaterials*. **131**, 111–120 (2017).

14. Baddeley, D., Bewersdorf, J. Biological Insight from Super-Resolution Microscopy: What We Can Learn from Localization-Based Images. *Annual Review of Biochemistry*. **87** (1), 965–989 (2018).
15. Ovesný, M., Křížek, P., Borkovec, J., Švindrych, Z., Hagen, G. M. ThunderSTORM: A comprehensive ImageJ plug-in for PALM and STORM data analysis and super-resolution imaging. *Bioinformatics*. **30** (16), 2389–2390 (2014).
16. Mahadev, K., Wu, X., Donnelly, S., Ouedraogo, R., Eckhart, A. D., Goldstein, B. J. Adiponectin inhibits vascular endothelial growth factor-induced migration of human coronary artery endothelial cells. *Cardiovascular Research*. **78** (2), 376–384 (2008).
17. Lemcke, H., Skorska, A., Lang, C. I., Johann, L., David, R. Quantitative evaluation of the sarcomere network of human hiPSC-derived cardiomyocytes using single-molecule localization microscopy. *International Journal of Molecular Sciences*. **21** (8), e2819 (2020)
18. Ackers-Johnson, M. et al. A simplified, langendorff-Free method for concomitant isolation of viable cardiac myocytes and nonmyocytes from the adult mouse heart. *Circulation Research*. **119** (8), 909–920 (2016).
19. Lemcke, H. et al. Applying 3D-FRAP microscopy to analyse gap junction-dependent shuttling of small antisense RNAs between cardiomyocytes. *Journal of Molecular and Cellular Cardiology*. **98**, 117–127 (2016).
20. Karbassi, E. et al. Cardiomyocyte maturation: advances in knowledge and implications for regenerative medicine. *Nature Reviews Cardiology*. **17** (6) 341-359 (2020).
21. Krysiak, J. et al. Protein phosphatase 5 regulates titin phosphorylation and function at a sarcomere-associated mechanosensor complex in cardiomyocytes. *Nature Communications*. **9** (1), 1–14 (2018).
22. Zaunbrecher, R. J. et al. Cronos Titin Is Expressed in Human Cardiomyocytes and Necessary for Normal Sarcomere Function. *Circulation*. **140** (20), 1647–1660 (2019).
23. Fornasiero, E. F., Opazo, F. Super-resolution imaging for cell biologists. *BioEssays*. eds Fornasiero, E. F., Opazo F. Wiley Online Library.(2015).
24. Jeziorowska, D. et al. Differential Sarcomere and Electrophysiological Maturation of Human iPSC-Derived Cardiac Myocytes in Monolayer vs. Aggregation-Based Differentiation Protocols. *International Journal of Molecular Sciences*. **18** (6), 1173 (2017).
25. Kroll, K. et al. Electro-mechanical conditioning of human iPSC-derived cardiomyocytes for translational research. *Progress in Biophysics and Molecular Biology*. **130**, 212–222 (2017).
26. Zuppinger, C. et al. Characterization of cytoskeleton features and maturation status of cultured human iPSC-derived cardiomyocytes. *European Journal of Histochemistry*. **61** (2), 145–153 (2017).
27. Jradi, F. M., Lavis, L. D. Chemistry of Photosensitive Fluorophores for Single-Molecule Localization Microscopy. *ACS Chemical Biology*. **14** (6), 1077–1090 (2019).
28. Dempsey, G. T., Vaughan, J. C., Chen, K. H., Bates, M., Zhuang, X. Evaluation of fluorophores for optimal performance in localization-based super-resolution imaging. *Nature Methods*. **8** (12), 1027–1036 (2011).
29. Lampe, A., Haucke, V., Sigrist, S. J., Heilemann, M., Schmoranzer, J. Multi-colour direct STORM with red emitting carbocyanines. *Biology of the Cell*. **104** (4), 229–237 (2012).
30. Chamma, I., Levet, F., Sibarita, J.-B., Sainlos, M., Thoumine, O. Nanoscale organization of synaptic adhesion proteins revealed by single-molecule localization microscopy.

572 *Neurophotonics*. **3** (4), 041810 (2016).
573 31. Ma, H., Fu, R., Xu, J., Liu, Y. A simple and cost-effective setup for super-resolution
574 localization microscopy. *Scientific Reports*. **7** (1), 1–9 (2017).
575 32. Olivier, N., Keller, D., Gönczy, P., Manley, S. Resolution Doubling in 3D-STORM Imaging
576 through Improved Buffers. *PLoS One*. **8** (7), e0069004 (2013).
577 33. Swoboda, M. et al. Enzymatic oxygen scavenging for photostability without ph drop in
578 single-molecule experiments. *ACS Nano*. **6** (7), 6364–6369 (2012).
579 34. Mikhaylova, M. et al. Resolving bundled microtubules using anti-tubulin nanobodies.
580 *Nature Communications*. **6** (1), 1–7 (2015).
581 35. Venkataramani, V. et al. Enhanced labeling density and whole-cell 3D dSTORM imaging
582 by repetitive labeling of target proteins. *Scientific Reports*. **8** (1), 1–7 (2018).
583 36. Erdélyi, M. et al. Origin and compensation of imaging artefacts in localization-based
584 super-resolution microscopy. *Methods*. **88**, 122–132 (2015).
585 37. McGorty, R., Schnitzbauer, J., Zhang, W., Huang, B. Correction of depth-dependent
586 aberrations in 3D single-molecule localization and super-resolution microscopy. *Optics Letters*.
587 **39** (2), 275 (2014).
588 38. Ribeiro, M. C. et al. A cardiomyocyte show of force: A fluorescent alpha-actinin reporter
589 line sheds light on human cardiomyocyte contractility versus substrate stiffness. *Journal of*
590 *Molecular and Cellular Cardiology*. **141**, 54–64 (2020).
591 39. Pioner, J. M. et al. Isolation and mechanical measurements of myofibrils from human
592 induced pluripotent stem cell-derived cardiomyocytes. *Stem Cell Reports*. **6** (6), 885–896 (2016).
593

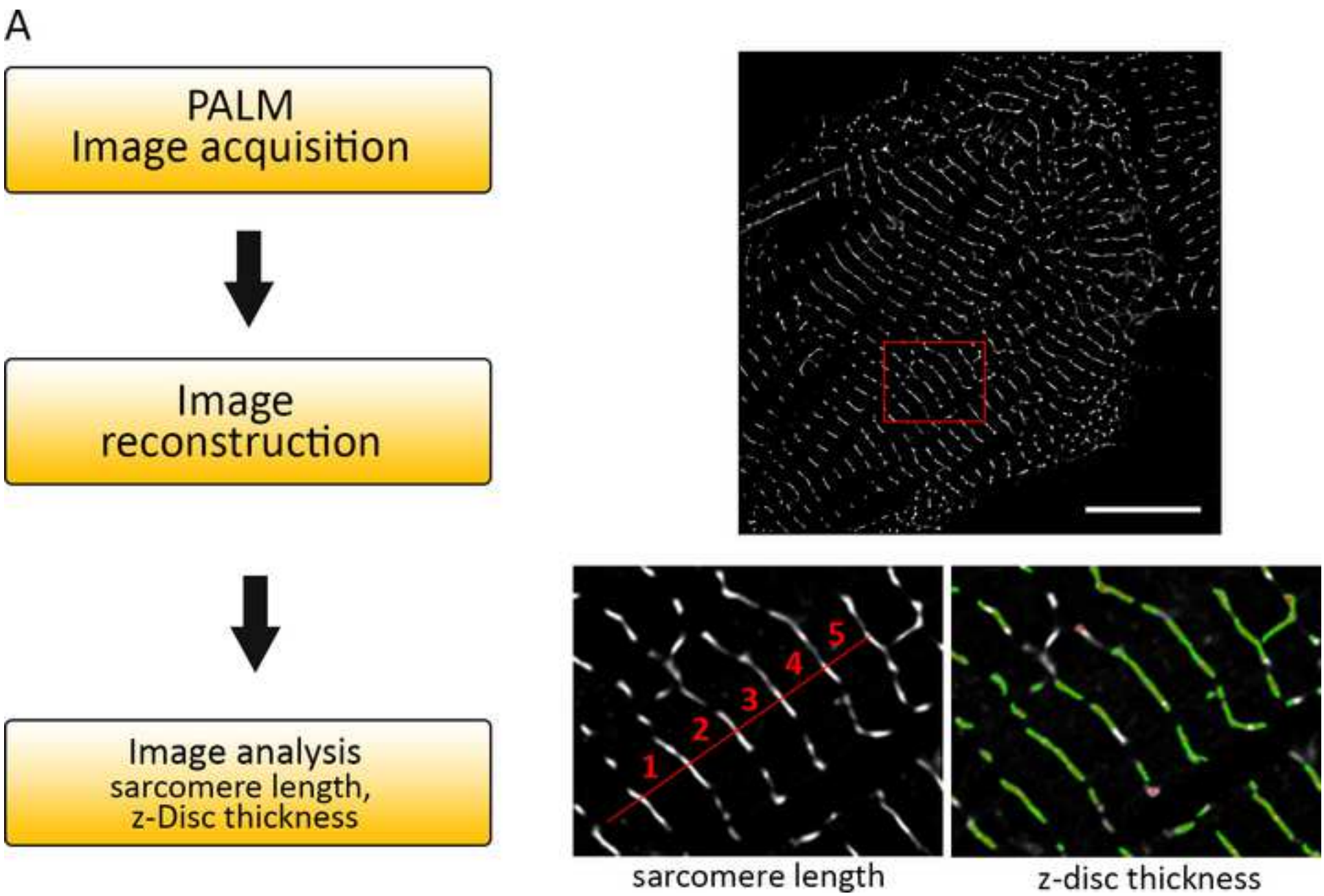

Figure 2

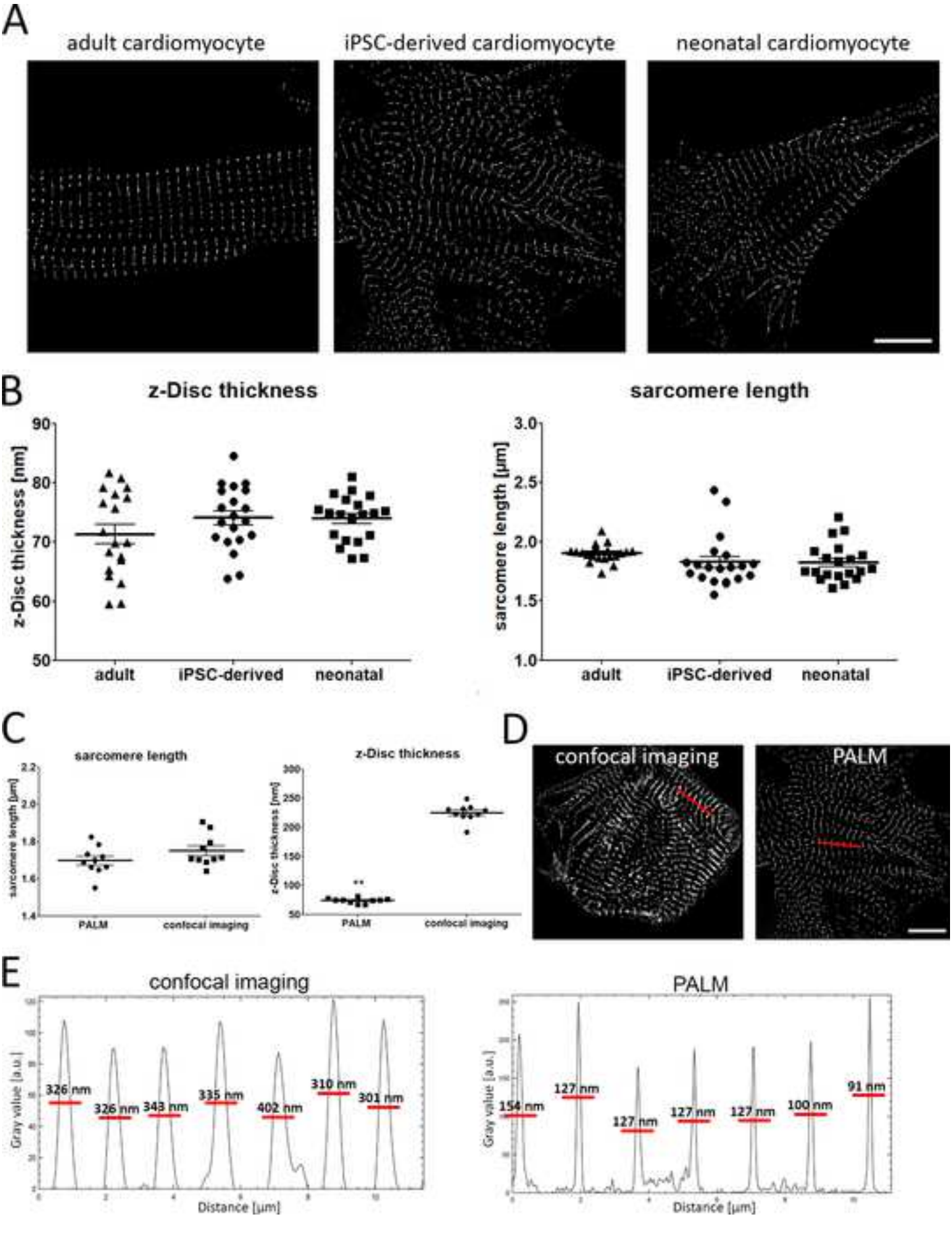

Figure 3

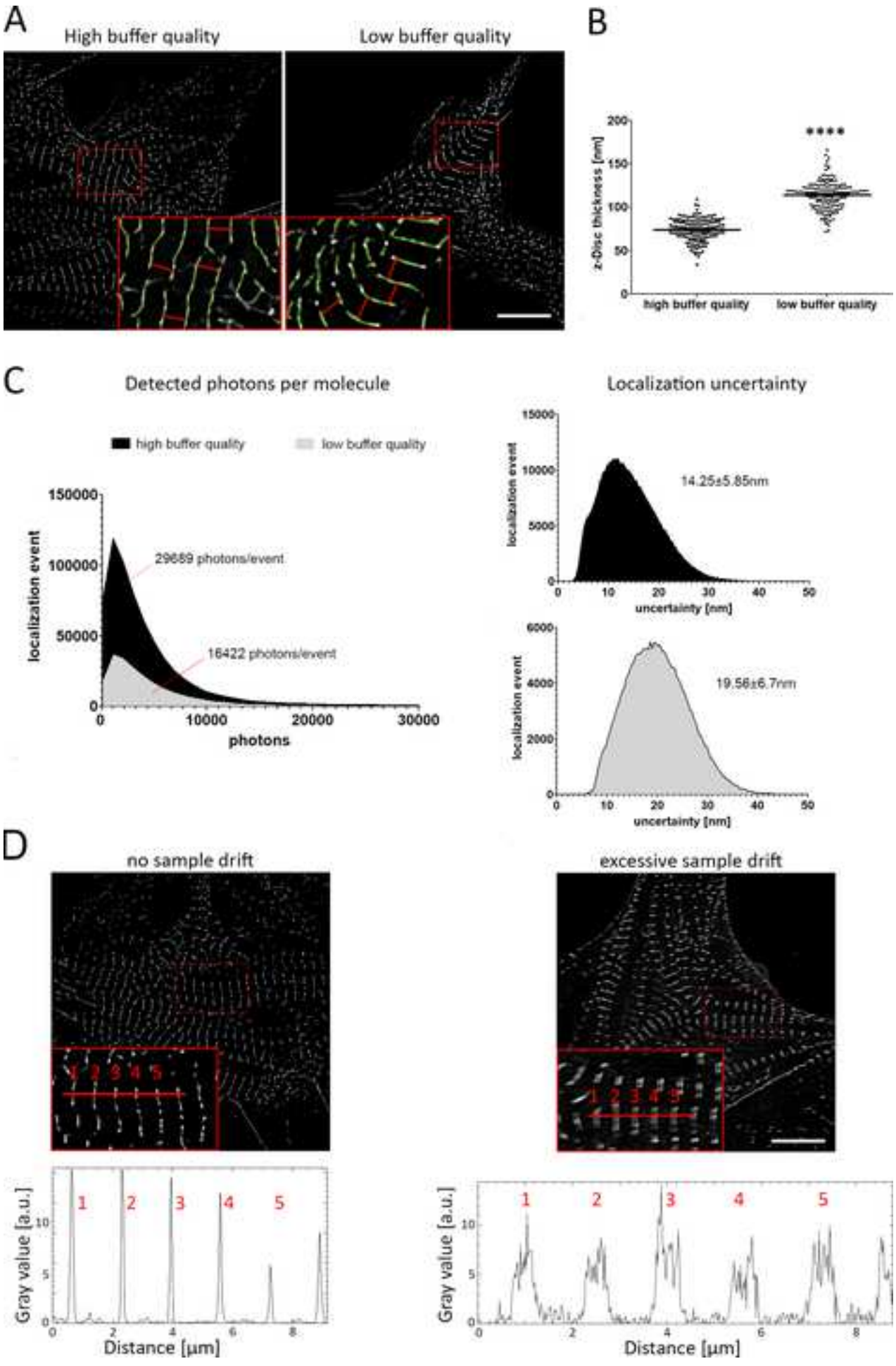

Table of Materials

Name of Material/ Equipment	Company	Catalog Number
human iPSC cell line	Takara	Y00325
µ-Slide 8 Well Glass Bottom	ibidi	80827
0.5ml eppendorf tube	Eppendorf	30121023
Bovine serum albumin	Sigma Aldrich	A906
Cardiomyocyte Dissociation Kit	Stem Cell Technologies	05025
Catalase	Sigma Aldrich	C40-1G
Cyclooctatetraene	Sigma Aldrich	138924-1G
Cysteamine	Sigma Aldrich	30070-10g
Dulbecco's phosphate-buffered saline without Ca2+ and Mg2+	Thermo Fisher	14190169
F(ab')2-Goat anti-Mouse IgG Alexa Fluor 647	Thermo Fisher	A-21237
Fiji image processing software (Image J)		
Glucose	Carl Roth	X997.2
Hydrochloric acid	Sigma Aldrich	H1758
LSM 780 ELYRA PS.1 system	Zeiss	
Paraformaldehyde	Merck	8187150100
Pyranose oxidase	Sigma Aldrich	P4234-250UN
sarcomeric α-actinin antibody [EA-53]	Abcam	ab9465
Sodium chloride	Sigma Aldrich	S7653
sterile water	Carl Roth	3255.1
Triton X-100	Sigma Aldrich	X100
Trizma base	Sigma Aldrich	T1503
β-Mercaptoethanol	Sigma Aldrich	63689

Comments/Description

Universität Rostock Traditio et Innovatio

Universitätsmedizin Rostock

Universitätsmedizin Rostock · PF 10 08 88 · 18055 Rostock

To the Editor

"*Journal of Visualized Experiments*"

Jaydev Upponi, Ph.D.

1 Alewife Center, Suite 200

Cambridge MA 02140, United States

22.06.2020

Klinik und Poliklinik für Herzchirurgie

im Perioperativen Zentrum (POZ)
Schillingallee 35, 18057 Rostock

Universitäres Herzzentrum Rostock

Referenz-und Translationszentrum für Kardiale Stammzelltherapie

im Biomedizinischen
Forschungszentrum (BMFZ)
Schillingallee 69, 18057 Rostock

RTC

Leiter:
Prof. Dr. med. habil. Gustav Steinhoff
Telefon: +49 381 494-6100
gustav.steinhoff@med.uni-rostock.de

Professur für Regenerative Medizin:
Prof. Dr. rer. nat. Robert David
Telefon: +49 381 498-8973
Telefax: +49 381 498-8970
robert.david@med.uni-rostock.de

Projektassistenz:
Mandy Klingbeil
Telefon: +49 381 498-8974
Telefax: +49 381 498-8970
610mandy.klingbeil@med.uni-rostock.de

Submission of our revised manuscript entitled

"Analyzing the α-actinin network in human iPSC-derived cardiomyocytes by application of single molecule localization microscopy"

(previous title: "Analyzing the structural maturation of human iPSC-derived cardiomyocytes using photoactivated localization microscopy)

Dear Dr. Upponi,

we appreciate the opportunity for revision of our manuscript and hereby re-submit it for publication in *Journal of Visualized Experiments*.

The editor and the reviewers have provided us with valuable suggestions to significantly further improve our work.

As suggested by the reviewers, we have performed additional experiments showing the sarcomere organization of adult cardiomyocytes, which allows better evaluation of the structural maturation of iPSC-derived cardiac cells.

In this regard, we have added new subfigures and modified the text in the results and discussion section. Further, we have included data showing the improved lateral resolution of PALM imaging for more accurate data acquisition.

Below please find our point-by-point responses to the issues raised by the editor and the reviewers that, we believe, are fully addressed in our revised manuscript. We therefore are highly confident that the manuscript can now be accepted for publication.

Sincerely,

Prof. Robert David, PhD

Editorial comments:

Changes to be made by the Author(s):

1. Please take this opportunity to thoroughly proofread the manuscript to ensure that there are no spelling or grammar issues. The JoVE editor will not copy-edit your manuscript and any errors in the submitted revision may be present in the published version. Please use American English throughout. done

2. Please format the manuscript as: paragraph Indentation: 0 for both left and right and special: none, Line spacings: single. Please include a single line space between each step, substep and note in the protocol section. Please use Calibri 12 points. done

3. Please ensure that the long Abstract is within 150-300-word limit and clearly states the goal of the protocol. done

4. Please revise and expand the Introduction to include all of the following with citation:

a) A clear statement of the overall goal of this method

b) The rationale behind the development and/or use of this technique

c) The advantages over alternative techniques with applicable references to previous studies

d) A description of the context of the technique in the wider body of literature

e) Information to help readers to determine whether the method is appropriate for their application

We have modified the introduction section to fulfill the criteria mentioned above, e.g. including a statement about the overall goal of the presented protocol.

5. Please ensure that all text in the protocol section is written in the imperative tense as if telling someone how to do the technique (e.g., “Do this,” “Ensure that,” etc.). The actions should be described in the imperative tense in complete sentences wherever possible. Avoid usage of phrases such as “could be,” “should be,” and “would be” throughout the Protocol. Any text that cannot be written in the imperative tense may be added as a “Note.” However, notes should be concise and used sparingly. done

6. The Protocol should contain only action items that direct the reader to do something. done

7. The Protocol should be made up almost entirely of discrete steps without large paragraphs of text between sections. done

8. Please ensure that individual steps of the protocol should only contain 2-3 actions sentences per step. done

9. Please ensure you answer the “how” question, i.e., how is the step performed? done

10. What kind of cells are used in the protocol? Significance?

We have used a human iPSC cell line, differentiated into cardiomyocytes. Adult and neonatal cardiomyocytes were isolated from NMRI mice. Since our protocol focuses on labelling and image analysis of the sarcomere network rather than on cell differentiation and isolation, we briefly explained the cell culture procedure and refer to previous publications that described cell cultivation and isolation in more detail (Protocol section 1.-3.)

11. 2.4.1- Is this 10 x g or 10, 000 x g? To avoid misunderstanding, we have removed the period.

12. Is thunderstorm plugin open access? Yes, the thunderstorm plugin is open source software.

13. Please use complete sentences to describe the action. done

14. There is a 10-page limit for the Protocol, but there is a 2.75-page limit for filmable content. Please highlight 2.75 pages or less of the Protocol (including headings and spacing) that identifies the essential steps of the protocol for the video, i.e., the steps that should be visualized to tell the most cohesive story of the Protocol. done

15. Please ensure the result are described with respect to your technique presented; you performed an experiment, how did it help you to conclude what you wanted to and how is it in line with the title. done
16. Please obtain explicit copyright permission to reuse any figures from a previous publication. Explicit permission can be expressed in the form of a letter from the editor or a link to the editorial policy that allows re-prints. Please upload this information as a .doc or .docx file to your Editorial Manager account. The Figure must be cited appropriately in the Figure Legend, i.e. "This figure has been modified from [citation]." No copyright permission is needed.
17. As we are a methods journal, please ensure that the Discussion explicitly cover the following in detail in 3-6 paragraphs with citations:
a) Critical steps within the protocol
b) Any modifications and troubleshooting of the technique
c) Any limitations of the technique
d) The significance with respect to existing methods
e) Any future applications of the technique
done
18. Please remove trademark (™) and registered (®) symbols from the Table of Equipment and Materials. Please sort the materials table in alphabetical order. done

Reviewers' comments:

Reviewer #1:

Manuscript Summary:
The manuscript provides a clear protocol, and the authors demonstrate that the protocol yields high resolution images of cardiomyocytes (CMs) which can subsequently be analyzed for parameters such as sarcomere length and z- disc thickness. The authors also demonstrate why adherence to the protocol is required to obtain high resolution images. However, the authors do not adequately contextualize the relevance and need for the protocol. Revisions to address such shortcomings are suggested and listed below.

Major Concerns:

1. *Reference to previous studies which demonstrate differences in sarcomere length and z-disk width in wild type vs. disease iPSC-derived CMs (such as Pioner et. al. Cardiovascular Research, 2020) as well as studies that demonstrate changes in sarcomere length as a result better maturation (such as Carson et. al. ACS Appl Master Interfaces, 2017) would justify using these parameters to assess maturation.*

   We appreciate the reviewer's suggestion and have added information why z-Disc thickness and sarcomere length are appropriate parameters to evaluate maturation, including respective references (line 81-85.)

2. *The authors claim that the comparison of sarcomere lengths for iPSC-derived CMs and neonatal CMs demonstrates the lack of maturation of the iPSC-derived CMs. Measurement of sarcomere length in mature CMs should be included to demonstrate that mature cardiomyocytes do have longer sarcomere lengths and that sarcomere length can therefore be used to assess maturation.*

   The reviewer is right that data from fully mature cardiomyocytes would allow better evaluation of the developmental state of iPSC-derived CMs. Therefore, we have included additional data of z-Disc thickness and sarcomere length measured in adult mature cardiomyocytes obtained from murine heart tissue (Figure 2A, B).

3. *The need for techniques such as PALM to investigate the sarcomere structure can be made stronger by citing previous studies that study the role of sarcomere structure/composition in cardiac disease such as Zaunbrecher et. al. Circulation, 2019*

   We thank the reviewer for his advice. We have included a statement in the discussion section to further highlight the importance of PALM for investigating the role of specific proteins for sarcomere function (412-414)

4. *In the introduction a lack of functional maturity of iPSC-CMs is mentioned, but a significant drawback of this method is the inability to collect functional parameters concerning cell contractility. Preemptively addressing this by citing studies that already accomplish this such as Miklas et. al. Circulation Research, 2020 and Pioner et. al. Stem Cell Reports, 2016 is needed to help clarify that this technique is addressing the need to improve the investigation of sarcomere structure instead of function.*

   The reviewer is right that the presented method does not allow acquisition of functional parameters, like contractility. We have added a paragraph describing these drawbacks and provide information about studies that have acquired both structural and functional data, although with much lower resolution (line 468-475)

5. *Comparison of sarcomere length and z-disk thickness measurements made via PALM vs. conventional/standard techniques are required to support the assertion that PALM yields more accurate analysis.*

   According to the reviewer´s suggestion, we have performed additional experiments to show the difference between conventional confocal imaging and PALM-based image acquisition. We have included these data in Figure 2 and modified the results and discussion section. Figure 2 C shows sarcomere length and z-Disc thickness acquired with both imaging techniques. Further we highlight the improved resolution of PALM by indicating the full width at half maximum of fluorescence intensity profile plots (Figure 2 D,E) (line 327-334, line 427-431)

Minor Concerns:

6. *In step 3.4.3 the authors suggest taking "5.000 to 10.000 frames." The use of a decimal/period makes it unclear as to whether the authors means "five to ten" or "five thousand to ten thousand" frames.*

   We have acquired 5000-10000 frames per PALM image. To avoid misunderstandings, we have removed the period.

7. *For step 5.1.2 it may be appropriate to mention specifically to draw the line perpendicular to the z-discs so that peaks in the resulting plot represent the shortest distance between the z-discs*

   As suggested by the reviewer, we have added the information regarding line drawing (line 287-288).

8. *In the zoomed in images in Figure 2 indicators such as arrows to indicate a representative measurement of sarcomere length and z-disc thickness would make it clearer what exactly is being measured, especially for the z-disc thickness as the image by itself does not make it clear whether the short/thin or longer/wider dimension of the z-disc is being measured.*

   We appreciate the reviewers´ suggestions. As Figure 2 does not contain any zoomed images, the reviewer´s comment obviously refers to Figure 3. We have now indicated representative measurements of sarcomere length by red lines. Also, filament structures used for calculating z-Disc thickness were labelled in green.

Reviewer #2:

Manuscript Summary:
Assessing the maturation level of iPSC derived cardiomyocytes (CMs) is essential for using and comparing CM models and the results obtained using them. The authors present a method for accurately imaging the CM key structural aspects, and measure sarcomere lengths and z-disc widths. The methods are generally well described. The process and results are easy to understand and follow.
I have only a few minor remarks to make.

Minor Concerns:

1. *Title: The study presents a method for analyzing the structural properties of human iPSC-derived CMs, which can be of use when assessing the maturity level of these cells, among other uses. The title in its current form is slightly misleading, as it suggests that CM maturity is analyzed, while the study does not include mature cell types or compare the results with previous studies. The title of the study should reflect this.*

   We agree with the reviewer that CM maturity is difficult to evaluate without a direct comparison with mature CM. Therefore, we have included data of z-Disc thickness and sarcomere length of

mature cardiomyocytes derived from adult mice (Figure 2) Also, we have changed the title that now focuses on analysis of the α-actinin sarcomere network.

2. *Introduction: The authors set a high bar for the scientific community when requiring identicalness: "researchers have failed to generate iPSC-derived CM, matching identical phenotypical and functional properties as their native counterparts." Animal models are very far from the humans in drug screening assays but are nevertheless used. Progress in the iPSC-CM field has certainly not been as fast as many would have hoped. However, "all models are wrong, but some are useful". The authors could revise this statement e.g. by indicating aspects of iPSC-CMs that hamper their in vitro use*.

   As suggested by the reviewer, we have modified the respective statement (line 61-62)

3. *The disorganized sarcomere structure not only causes reduced ability of cell contraction, but also influences the entire contraction dynamics: the uniaxial contraction of mature cells is replaced by the radial contraction and contraction focal points in immature cells. This is briefly mentioned by the authors in the second to last paragraph in discussion, but the orientation issue should be raised in introduction as well.*

   We appreciate the reviewers comment. We have added information about the orientation of sarcomere filaments in immature CM and their impact on cell contraction dynamics (line67-70).

4. *Protocol/table of materials: The study does not indicate the origin of the iPSC-CM cell line and the animal from which the neonatal cells are excised from. Although the study aims to present the method and not the cells, hIPSC-CM culture and differentiation protocol should be documented in some way as well, as the measurement results are compared with literature values.*

   We thank the reviewer for his advice. Origin of the iPSC cell line is now given in the table of materials. Origin of neonatal and adult cardiomyocytes is mentioned in the protocol section (2.1, 3.1). As already stated by the reviewer, our protocol focuses on the imaging technique rather than on cell culture methods. Thus, we briefly introduced cultivation and isolation of hiPSC-CM and native CM and refer to previously published studies that describe the process of isolation and cultivation in more detail.

5. *Results: Please indicate in text the N and measure of variation in text, as now it is mentioned only in figure captions.*

   We have added the respective information in the results section.

6. *Discussion: In line with my previous remark regarding the title, I would suggest rewording the last paragraph to better fit the study. While the measured parameters are very important aspects in assessing sarcomere properties, CM structural maturity consists of more aspects, such as*

remodeling of nuclei and other organelles, development of T-tubules, increase in myofibril content.

We have modified the title and discussion section according to the reviewer's suggestions. We now describe our method as a tool to particularly characterize the maturation state of the sarcomere/α-actinin network in CM, rather than a tool to evaluate structural maturation in general (line 327).

Reviewer #3:

Manuscript Summary:
The manuscript describes a microscopy approach to monitoring cardiomyocyte sarcomeres with high resolution. The sarcomere images are very clear and the procedural details are present. There are concerns however that reduce enthusiasm for publication

Major Concerns:

1. *There is no detail about the cardiomyocytes used for the study. What is the source of the neonatal cells? What is the source of the hiPSC-CMs?*

   We thank the reviewer for his comment. We have added information regarding source of neonatal mice and origin of hiPSC-CM in the protocol section (1.-3.) and table of materials. Since our protocol focuses on the imaging technique, we briefly described the process of isolation and cultivation of cells and refer to previous studies that provide more detailed information of cardiac differentiation and cell isolation.

2. *Also, there is no application of the procedure to study maturation-the process that this approach is suppose to enable study of.*

   We appreciate the reviewer´s comment. We did not intend to provide a strategy in order to improve the maturation of iPSC-derived CM. Instead, the purpose of the study was to demonstrate our method as tool to evaluate the sarcomere maturation. To further support this conclusion, we included data of mature CM for the direct comparison of z-Disc thickness and sarcomere length between neonatal, adult and iPSC-CM (Figure 2). These data show that our approach is suitable to characterize the sarcomere network at different developmental stages and thus in the future can be applied to analyze the efficiency of protocols/strategies aiming to improve sarcomere maturation.

Minor Concerns:

3. *It is not clear how this new microscopy approach is an improvement over using FFT analysis of phase contrast or confocal images. There are other methods available to determine maturation of hiPSC-CMs that do not require fixation and processing. Further, there are live cell staining approaches using fluorescent labelled actin and actinin to probe maturation in living cells.*

We agree with the reviewer that several methods are available to analyze the maturation process of iPSC-CM. However, compared to conventional confocal imaging, PALM gives significantly improved spatial resolution that allows increased data accuracy. This is in particular important when subtle alterations of the sarcomere network need to be detected.
Also, the reviewer is right that live cell imaging with fluorescently labelled actinin also represents a technique that can be applied to obtain structural and functional data, although spatial resolution is much reduced. Due to the long acquisition process our microscopy approach is less appropriate for live cell imaging. Yet, our approach provides the possibility to be combined with previous time lapse recordings in order to correlate PALM data with functional parameters like contraction capacity. We have included this information in the discussion section and mentioned the drawbacks of our method. (line 457, 468-475)